Superconducting and normal state properties of the systems $La_{1-x}M_xPt_4Ge_{12}$ ($M =$ Ce, Th)

K. Huang,[1,2,3,*] D. Yazici,[1,2,†] B. D. White,[1,2,‡] I. Jeon,[2,3] A. J. Breindel,[1,2] N. Pouse,[1,2] and M. B. Maple[1,2,3,§]

[1]*Department of Physics, University of California, San Diego, La Jolla, California 92093, USA*
[2]*Center for Advanced Nanoscience, University of California, San Diego, La Jolla, California 92093, USA*
[3]*Materials Science and Engineering Program, University of California, San Diego, La Jolla, California 92093, USA*

Electrical resistivity, magnetization, and specific heat measurements were performed on polycrystalline samples of the filled-skutterudite systems $La_{1-x}M_xPt_4Ge_{12}$ ($M =$ Ce and Th). Superconductivity in $LaPt_4Ge_{12}$ was quickly suppressed with Ce substitution and no evidence for superconductivity was found down to 1.1 K for $x > 0.2$. Temperature-dependent specific heat data at low temperatures for $La_{1-x}Ce_xPt_4Ge_{12}$ show a change from power-law to exponential behavior, which may be an indication for multiband superconductivity in $LaPt_4Ge_{12}$. A similar crossover was observed in the $Pr_{1-x}Ce_xPt_4Ge_{12}$ system. However, the suppression rates of the superconducting transition temperatures $T_c(x)$ in the two systems are quite disparate, indicating a difference in the nature of superconductivity, which is conventional in $LaPt_4Ge_{12}$ and unconventional in $PrPt_4Ge_{12}$. In comparison, a nearly linear and smooth evolution of T_c with increasing Th was observed in the $La_{1-x}Th_xPt_4Ge_{12}$ system, with no change of the superconducting energy gap in the temperature dependence of the specific heat, suggesting similar types of superconductivity in both the $LaPt_4Ge_{12}$ and $ThPt_4Ge_{12}$ compounds.

I. INTRODUCTION

Recently, a new branch of filled skutterudites was discovered with the chemical formula APt_4Ge_{12} [1,2]. Several members of this branch were found to exhibit superconductivity with $A =$ La and Pr exhibiting the highest superconducting transition temperatures, $T_c \sim 8$ K [1–3]. Considerable attention has been focused on $PrPt_4Ge_{12}$ as it exhibits signs of unconventional superconductivity [4–10]. However, investigations into $SrPt_4Ge_{12}$ and $BaPt_4Ge_{12}$ show that the superconductivity is conventional BCS-type which originates from, and is intrinsic to, the Pt-Ge cages [1]. Furthermore, $LaPt_4Ge_{12}$ was also found to exhibit evidence for conventional BCS-type superconductivity from nuclear magnetic resonance (NMR) and ^{73}Ge nuclear quadrupole resonance (NQR) measurements [11,12].

The compound $CePt_4Ge_{12}$ is thought to lie on the border between an intermediate-valence (IV) and a Kondo lattice compound [11]. Initial investigations into $CePt_4Ge_{12}$ revealed a broad maximum in the magnetization $M(T)$, which can be a characteristic of intermediate-valence compounds. However, high-resolution x-ray absorption spectroscopy measurements indicated that the Ce ions exhibit a temperature-independent valence close to $\sim 3^+$ [13]. Recent inelastic neutron scattering measurements find a wider quasielastic peak at higher energies, consistent with an IV system, as well as the absence of crystalline electric field effects expected in a Kondo system [14].

Therefore we decided to investigate the $La_{1-x}Ce_xPt_4Ge_{12}$ system to complement our previous study of the $Pr_{1-x}Ce_xPt_4Ge_{12}$ system. We anticipated that these two investigations could provide valuable insight into the nature of superconductivity in the Pt-Ge based filled skutterudites. Additionally, studies of $ThPt_4Ge_{12}$ have uncovered signatures of an exotic form of superconductivity from μSR measurements [15], power-law contributions to specific heat [16], and a complex Fermi surface from band-structure calculations [17]; these results motivated a parallel study on the system $La_{1-x}Th_xPt_4Ge_{12}$.

We found that T_c in $La_{1-x}Ce_xPt_4Ge_{12}$ is suppressed rapidly and almost linearly with increasing x, with the onset of superconductivity no longer being observable down to 1.1 K for $x \geqslant 0.2$. In contrast, the onset of superconductivity in $Pr_{1-x}Ce_xPt_4Ge_{12}$ persists up to $x = 0.5$, and the T_c versus x curve has pronounced positive curvature [9]. In the $La_{1-x}Th_xPt_4Ge_{12}$ system, we observed a smooth and continuous change in T_c versus x, which is inconsistent with the behavior that would be expected for the existence of different types of superconducting states [18,19]; i.e., the continuous and smooth behavior of T_c versus x instead suggests that both $LaPt_4Ge_{12}$ and $ThPt_4Ge_{12}$ exhibit the same type of superconductivity.

A change in the temperature dependence of the specific heat in the superconducting state of $La_{1-x}Ce_xPt_4Ge_{12}$ is observed; this may be evidence for a crossover from multiband superconductivity in $LaPt_4Ge_{12}$ to isotropic single-band superconductivity in the $x > 0$ samples. A similar crossover in the specific heat behavior was observed when Ce was substituted into $PrPt_4Ge_{12}$, a material with well-established evidence for multiband superconductivity [6–9]. Specific heat measurements on the system $La_{1-x}Th_xPt_4Ge_{12}$ from $x = 0$ to $x = 0.2$ did not exhibit a similar change. Taken together with previous studies, it is possible that both $LaPt_4Ge_{12}$ and $ThPt_4Ge_{12}$ are multiband superconductors.

_____

*Present address: Department of Physics, Fudan University, Shanghai 200433, China.

†Present address: Faculty of Health Sciences, Artvin Coruh University, Artvin 08100, Turkey.

‡Present address: Department of Physics, Central Washington University, Ellensburg, Washington 98926-7442, USA.

§Corresponding author: mbmaple@ucsd.edu

II. EXPERIMENTAL DETAILS

Polycrystalline samples of $La_{1-x}Ce_xPt_4Ge_{12}$ ($x = 0$, 0.05, 0.1, 0.15, 0.2, 0.4, 0.6, 0.80, 1) and $La_{1-x}Th_xPt_4Ge_{12}$ ($x = 0$,

0.2, 0.4, 0.6, 0.8, 1) were synthesized in an atmosphere of ultrahigh-purity argon by arc-melting in a custom built arc furnace employing a zirconium getter on a water-cooled copper hearth. The starting materials were La ingots (Sigma-Aldrich, 99.9%), Ce rods (Alfa Aesar 3N, EPSI 99.9%), Th pieces, Pt sponge arc-melted into spheres (99.9999+%), and Ge pieces (Alfa Aesar 99.9999+%). The starting materials were weighed out in the molar stochiometric ratios, arc-melted together, and then flipped over and arc-melted again four more times to promote homogeneity. All samples were heat treated in a sealed quartz tube under an inert atmosphere (200 torr Ar) for 336 hours at 800 °C.

Powder x-ray diffraction (XRD) measurements were performed using a Bruker D8 x-ray diffractometer with a Cu K_α source. Four-wire electrical resistivity measurements were performed from 300 K down to ∼1.1 K in a pumped ^{4}He Dewar. Magnetization measurements were performed between 300 and 2 K in a Quantum Design Magnetic Property Measurement System (MPMS) equipped with a 7-T superconducting magnet. Specific heat measurements were performed down to 1.8 K using a Quantum Design Physical Property Measurement System (PPMS) DynaCool. The heat capacity measurements employed a standard thermal relaxation technique.

III. RESULTS

Rietveld refinements were performed on the powder XRD patterns for each sample using GSAS [20] and EXPGUI [21]. Displayed in Fig. 1(a) is an XRD pattern for La$_{0.4}$Ce$_{0.6}$Pt$_4$Ge$_{12}$, representative of the XRD patterns observed for values of x throughout both the La$_{1-x}$Ce$_x$Pt$_4$Ge$_{12}$ and La$_{1-x}$Th$_x$Pt$_4$Ge$_{12}$ systems. The blue line is the experimental XRD pattern and

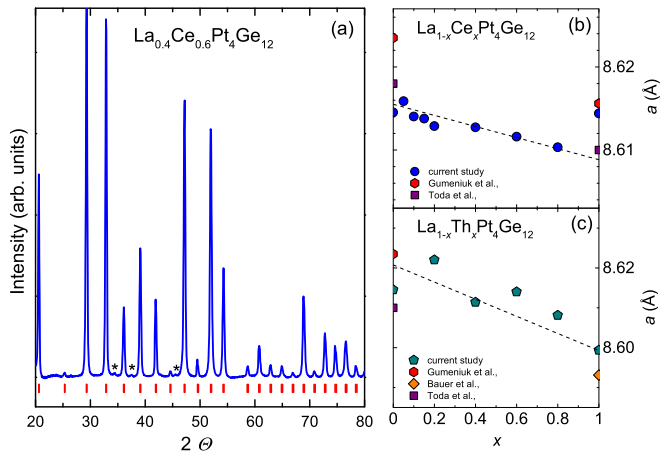

FIG. 1. (a) Powder x-ray diffraction pattern for a representative sample of La$_{1-x}$Ce$_x$Pt$_4$Ge$_{12}$ ($x = 0.6$) where the blue line represents the intensity versus 2Θ and the red tick marks locate the 2Θ positions of the expected Bragg reflections for the refined filled-skutterudite crystal structure. Black asterisks indicate Bragg reflections associated with a Ge/PtGe$_2$ impurity phase. The lattice parameter, a, is plotted for La$_{1-x}$Ce$_x$Pt$_4$Ge$_{12}$ in (b) and for La$_{1-x}$Th$_x$Pt$_4$Ge$_{12}$ in (c). The dashed lines are guides to the eye. The a versus x data for both La$_{1-x}$Ce$_x$Pt$_4$Ge$_{12}$ and La$_{1-x}$Th$_x$Pt$_4$Ge$_{12}$ obey Vegard's law, except for $x = 1$, in La$_{1-x}$Ce$_x$Pt$_4$Ge$_{12}$, where a has a larger value (see text). The a values for LaPt$_4$Ge$_{12}$, CePt$_4$Ge$_{12}$, and ThPt$_4$Ge$_{12}$ are plotted for comparison.

the red tick marks below locate the 2Θ positions of the expected Bragg reflections for the refined filled-skutterudite crystal structure. The cubic filled-skutterudite crystal structure (space group $Im\bar{3}$) was observed over the entire range of x for both series. As is commonly observed in the Pt-Ge based skutterudites [2,7,8,11,14,22,23], small impurity phases of Ge and/or PtGe$_2$ (at most up to ∼5% by mass) were detected in the samples. Figures 1(b) and 1(c) display the lattice parameter a for La$_{1-x}$Ce$_x$Pt$_4$Ge$_{12}$ (blue circles) and La$_{1-x}$Th$_x$Pt$_4$Ge$_{12}$ (teal pentagons) with dashed lines serving as guides to the eye. The system La$_{1-x}$Th$_x$Pt$_4$Ge$_{12}$ exhibits a linear decrease of a as x increases with the end members exhibiting a values of 8.618 Å for $x = 0$ and 8.615 Å for $x = 1$. The plot of a versus x for La$_{1-x}$Ce$_x$Pt$_4$Ge$_{12}$ shows a sudden increase in a of about 0.3% at $x = 1$. This may be because the XRD measurements for the sample with $x = 1$ were made using a different x-ray diffractometer. Another possible explanation for the larger a value for the sample with $x = 1$ is that there is a known sample dependence in the Pt-Ge based filled skutterudites; reported values for a of MPt$_4$Ge$_{12}$ ($M =$ La, Pr, Nd, Ce) differ by roughly 0.5% [2,11].

The electrical resistivity $\rho(T)$, measured in zero applied magnetic field, is displayed for the series La$_{1-x}$Ce$_x$Pt$_4$Ge$_{12}$ in Fig. 2(a) and La$_{1-x}$Th$_x$Pt$_4$Ge$_{12}$ in Fig. 2(b). The system La$_{1-x}$Ce$_x$Pt$_4$Ge$_{12}$ exhibits an overall increase in $\rho(T)$ with increasing x, except for $x = 1$ at low temperature, which exhibits a large decrease below 150 K. The overall shape of $\rho(T)$ exhibits the behavior of a simple metal, while at higher temperature, it has a negative curvature. This type of $\rho(T)$ behavior is often observed in the Ce-based filled skutterudites such as CeFe$_4$Sb$_{12}$ [24]. However, for La$_{1-x}$Th$_x$Pt$_4$Ge$_{12}$, $\rho(T)$ does not exhibit any clear trend with increasing x, possibly due to uncertainties in the measurement of the geometrical factors of the resistivity samples. Plotted in Fig. 2(c) are the scaled $\rho(T)$ data for the system La$_{1-x}$Ce$_x$Pt$_4$Ge$_{12}$ such that the slopes, $d\rho/dT$, are identical to $d\rho/dT$ for LaPt$_4$Ge$_{12}$ at high temperature. The scaled $\rho(T)$ data clearly show that additional electron scattering associated with the 4f electrons is introduced by Ce substitution. In contrast, when the same procedure is performed on the $\rho(T)$ data for La$_{1-x}$Th$_x$Pt$_4$Ge$_{12}$, displayed in Fig. 2(d), the scaled $\rho(T)$ data collapse onto a single curve, suggesting that Th substitution does not introduce any additional mechanisms for scattering electrons. The intrinsic differences in the $\rho(T)$ curves in Fig. 2(b) are due to differences in lattice scattering (electron-phonon scattering depends on the Debye temperature, $\Theta_D = 220$ K [13], in the Bloch-Grüneisen formula), and the nonmonotonic trend of the unscaled ρ at 300 K may be a consequence of errors in estimating the geometrical factor for the $x = 0.4, 0.6,$ and 0.8 samples.

For the La$_{1-x}$Ce$_x$Pt$_4$Ge$_{12}$ and La$_{1-x}$Th$_x$Pt$_4$Ge$_{12}$ series, the $\rho(T)$ data are well described by $\rho(T) = \rho_0 + AT^2$ up to ∼250 K^2 in Figs. 3(c) and 3(d), indicating that both systems exhibit Fermi liquid behavior. A is a fitting parameter and ρ_0 is the residual resistivity. The insets in Figs. 2(a) and 2(b) plot the residual resistivity ratio (RRR) as a function of x for La$_{1-x}$Ce$_x$Pt$_4$Ge$_{12}$ and La$_{1-x}$Th$_x$Pt$_4$Ge$_{12}$, respectively, where the RRR is defined as ρ_{300}/ρ_0, where ρ_{300} is the value of ρ at 300 K. The RRR versus x exhibits a parabolic shape with the minimum at $x = 0.6$ for both La$_{1-x}$Ce$_x$Pt$_4$Ge$_{12}$ (RRR = 3)

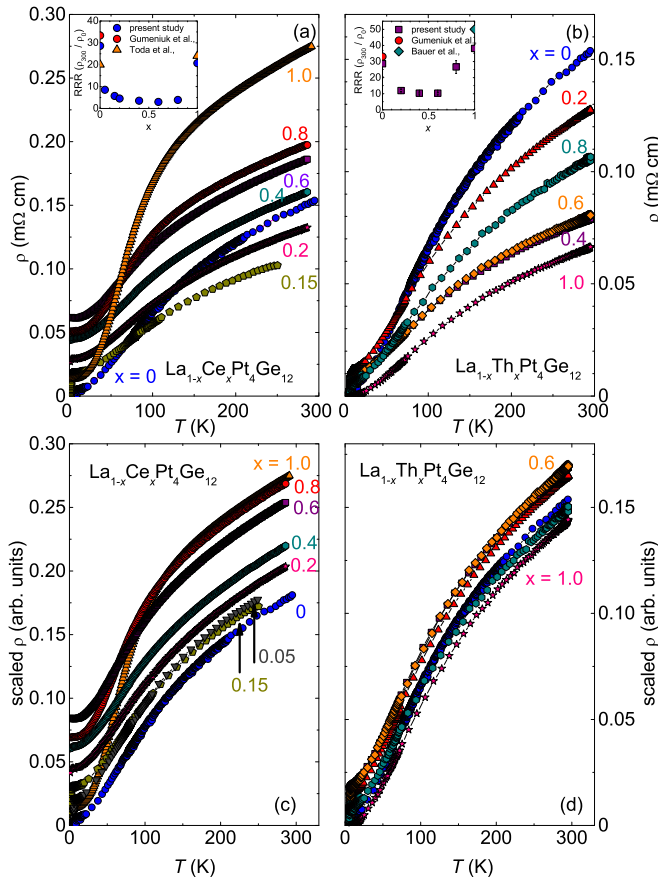FIG. 2. (a) Electrical resistivity ρ versus temperature T for La$_{1-x}$Ce$_x$Pt$_4$Ge$_{12}$. The electrical resistivity at high temperature is enhanced with increasing Ce concentration. The inset displays the residual resistivity ratio RRR (ρ_{300}/ρ_0) versus x for La$_{1-x}$Ce$_x$Pt$_4$Ge$_{12}$ (blue circles for this work), plotted as a function of x. The ratio exhibits a parabolic behavior with a minimum RRR = 3 for $x = 0.6$. (b) ρ versus T for La$_{1-x}$Th$_x$Pt$_4$Ge$_{12}$ which tends to exhibit an overall decrease of ρ with increasing x. The RRR versus x is displayed in the inset for La$_{1-x}$Th$_x$Pt$_4$Ge$_{12}$ (purple squares) with the minimum RRR = 10 at $x = 0.6$, similar to the parabolic behavior observed in La$_{1-x}$Ce$_x$Pt$_4$Ge$_{12}$. (c) Scaled $\rho(T)$ data for La$_{1-x}$Ce$_x$Pt$_4$Ge$_{12}$ such that the high-temperature slope $d\rho/dT$ matches the high-temperature $d\rho/dT$ of LaPt$_4$Ge$_{12}$. (d) Scaled $\rho(T)$ data for the La$_{1-x}$Th$_x$Pt$_4$Ge$_{12}$ system. The curves appear to collapse onto a single curve.

and La$_{1-x}$Th$_x$Pt$_4$Ge$_{12}$ (RRR = 10), close to the predicted minimum for simple alloys at $x = 0.5$.

There are clear drops in $\rho(T)$ at T_c. To determine T_c, the ratio $\rho(T)/\rho_{10}$, where ρ_{10} is $\rho(T = 10$ K) (a representative value of $\rho(T)$ in the normal state) was plotted versus T in Figs. 3(a) and 3(b) for La$_{1-x}$Ce$_x$Pt$_4$Ge$_{12}$ and La$_{1-x}$Th$_x$Pt$_4$Ge$_{12}$, respectively. T_c was defined as the temperature where $\rho(T)/\rho_{10} = 0.5$ and the width of the transition was characterized by the temperatures where $\rho(T)/\rho_{10} = 0.9$ and 0.1. For La$_{1-x}$Ce$_x$Pt$_4$Ge$_{12}$, T_c is rapidly suppressed with increasing x, with only the onset of superconductivity observed for $x = 0.2$ from measurements down to 1.1 K. In the system La$_{1-x}$Th$_x$Pt$_4$Ge$_{12}$, T_c is also suppressed with increasing x, from 8.3 K for $x = 0$ down to 4.5 K for $x = 1$. Th substitution suppresses T_c less rapidly than Ce substitution; however, this
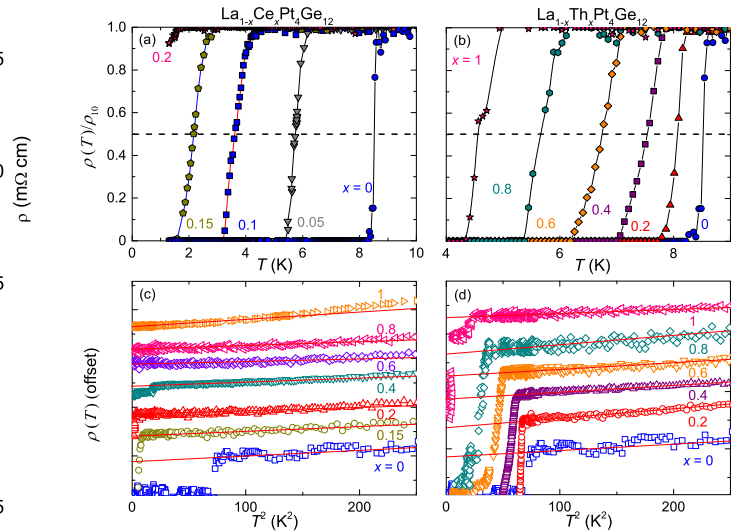

FIG. 3. The electrical resistivity normalized by ρ at $T = 10$ K, $\rho(T)/\rho_{10}$, versus T for La$_{1-x}$Ce$_x$Pt$_4$Ge$_{12}$ in (a) and La$_{1-x}$Th$_x$Pt$_4$Ge$_{12}$ in (b). The superconducting critical temperature T_c, where T_c is defined as $\rho(T)/\rho_{10} = 0.5$, for both systems decreases with increasing x. Measurements down to 1.1 K reveal that the onset of superconductivity is observable up to $x = 0.2$ for La$_{1-x}$Ce$_x$Pt$_4$Ge$_{12}$. The T_c for La$_{1-x}$Th$_x$Pt$_4$Ge$_{12}$ decreases almost linearly with x, with the lowest value of $T_c = 4.5$ K observed for $x = 1.0$, close to the reported value [3,16]. Selected ρ versus T^2 data for (c) La$_{1-x}$Ce$_x$Pt$_4$Ge$_{12}$ and (d) La$_{1-x}$Th$_x$Pt$_4$Ge$_{12}$ with offsets for visual clarity. Linear fits of $\rho(T) = \rho_0 + AT^2$ were performed up to roughly 250 K^2.

is not surprising since its $5f$ electron shell is empty so that Th is nonmagnetic and ThPt$_4$Ge$_{12}$ exhibits superconductivity. In contrast, CePt$_4$Ge$_{12}$ exhibits no ordered state down to 50 mK [11,13,25].

Magnetization divided by magnetic field, M/H, versus T data for La$_{1-x}$Ce$_x$Pt$_4$Ge$_{12}$ are shown in Fig. 4(a) where the $M(T)/H$ data were scaled by a factor of 1000 for clarity. $M(T)/H$ exhibits Curie-Weiss behavior above 200 K for all x and passes through a broad maximum around 80 K, followed by an upturn as $T \rightarrow 0$ K. The deviations from Curie-Weiss behavior, manifested by the broad maxima, could be an indication of either intermediate-valence (IV) behavior of Ce or Kondo lattice behavior [2]. The broad maxima become smaller in amplitude and width as the peak position shifts to lower temperatures with decreasing x, as seen in Fig. 4(c). This behavior may suggest that the local Kondo temperature, T_K, also decreases with decreasing x and that the $4f$ electrons are well localized at high temperatures. If T_K arises from the fully trivalent Ce^{3+}, then La substitution would weaken the Ce-Ce interactions, which would suppress the broad maxima as well as T_K. However, it should be noted that this behavior differs from that observed for La substitution into the compound CeRu$_4$Sb$_{12}$, where the broad maximum in $M(T)$ does not shift in temperature with increasing La concentration [26]. The small upturns in $M(T)/H$ as $T \rightarrow$ 0 K do not scale with x, making the upturns more likely due to small amounts of paramagnetic impurities, as described in previous literature [9,10,27], instead of being a signature of non-Fermi liquid behavior [28]. Both χ_{300}, $M(T)/H$ at
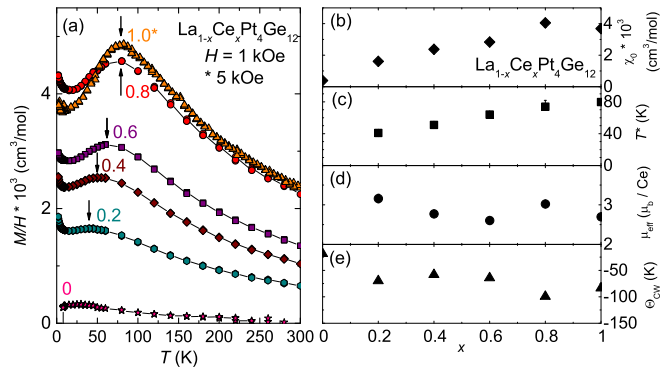
FIG. 4. (a) Magnetization divided by applied magnetic field, M/H, versus T from 300 K down to 2 K for the $La_{1-x}Ce_xPt_4Ge_{12}$ system. The magnetic susceptibility, $\chi(T) = M(T)/H$, increases with increasing x, exhibiting an almost tenfold increase between $x = 0$ and 1. (b) The low-temperature magnetic susceptibility χ_0, plotted as a function of x. χ_0 was determined by extrapolating $M(T)/H$ data to $T \rightarrow 0$ K while ignoring the small upturns observed at the lowest temperatures; these were determined to be due to small amounts of paramagnetic impurities. (c) T^*, the temperature where the broad maximum in the M/H versus T data is centered as indicated by the black arrows in (a), plotted versus x. The local maximum is possible evidence for either intermediate valence Ce or Kondo lattice behavior. T^* shifts to higher temperatures with increasing x, up to 80 K at $x = 1$, consistent with reported literature for $CePt_4Ge_{12}$ [11]. The effective magnetic moment μ_{eff} and Curie-Weiss temperature θ_{CW} were determined from Curie-Weiss fits performed on the inverse M/H data in the temperature range 200–300 K and are plotted versus x in (d) and (e), respectively.

300 K, and χ_0, $M(T)/H$ as $T \rightarrow 0$ K, are enhanced with increasing x. χ_{300} increases from ~ 0 cm^3/mol for $x = 0$ to 2.3×10^{-3} cm^3/mol for $x = 1$. χ_0 was determined by extrapolating $M(T)/H$ as $T \rightarrow 0$ K from data at temperatures above those where the broad upturns are observed. As can be seen in Fig. 4(b), χ_0 increases with increasing x, exhibiting an almost tenfold increase from $\chi_0 = 0.39 \times 10^{-3}$ cm^3/mol for $x = 0$ up to $\chi_0 = 3.69 \times 10^{-3}$ cm^3/mol for $x = 1$.

Curie-Weiss law fits were performed on the $M(T)/H$ data between 200 and 300 K for $La_{1-x}Ce_xPt_4Ge_{12}$; this temperature range was used because the broad maxima in $M(T)/H$ made fitting to lower temperatures inappropriate. The effective magnetic moment μ_{eff} and Curie-Weiss temperature θ_{CW} for $La_{1-x}Ce_xPt_4Ge_{12}$ were determined using the relation $M(T)/H = C_0/(T - \theta_{CW})$, where $C_0 = \mu_{eff}^2 N_A/3k_B$, N_A is Avagadro's number and k_B is Boltzmann's constant. The values we obtained for μ_{eff} and θ_{CW} are plotted in Figs. 4(d) and 4(e), respectively. $\mu_{eff} = 2.67$ μ_B/Ce for $x = 1$, which is slightly larger than the predicted value of 2.54 μ_B for the Ce^{3+} electronic configuration using Hund's rules; the limited temperature range for the Curie-Weiss fits, caused by the broad maximum, is possibly responsible for the disparity between the measured and calculated μ_{eff} values. The effective moment μ_{eff} increases slowly with decreasing x and exhibits values close to the free ion values derived from Hund's rules, reaching 3.16 μ_B/Ce for $x = 0.2$. The Curie-Weiss temperature $\theta_{CW} = -83$ K of $CePt_4Ge_{12}$ has a magnitude about twice as large as the value originally reported ($\theta_{CW} = -39.2$ K) [13],
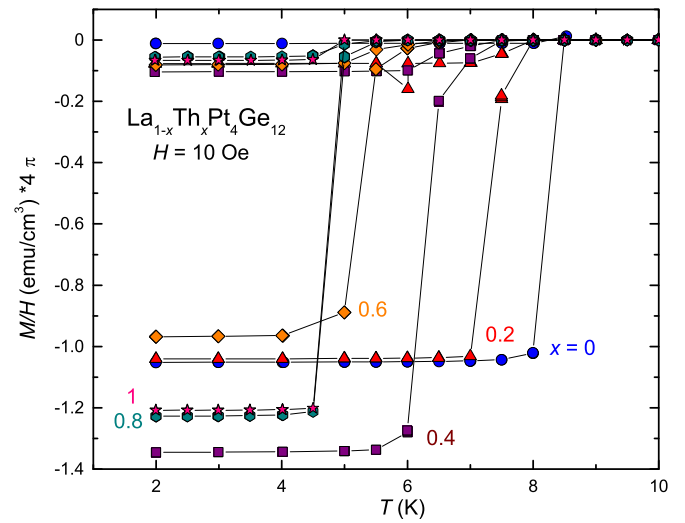

FIG. 5. Magnetization divided by magnetic field plotted as $4\pi M/H$ versus T for $La_{1-x}Th_xPt_4Ge_{12}$ from 2–10 K in an external magnetic field $H = 10$ Oe. The superconducting critical temperature T_c decreases as x increases, from 8 K for $x = 0$ down to 4.3 K for $x = 1$. The nearly unity value of $|4\pi M/H|$ is evidence for bulk superconductivity throughout the $La_{1-x}Th_xPt_4Ge_{12}$ series.

and within the scatter of the data, remains nearly constant with a value of -80 K throughout the entire series.

$M(T)/H$ measurements were performed for $La_{1-x}Th_xPt_4Ge_{12}$ samples in an applied magnetic field $H = 10$ Oe to determine T_c and the superconducting volume fraction, v, as can be seen in Fig. 5. The superconducting volume fraction, v, was estimated using the equation $M(T)/H \times d = v$, where $M(T)/H$ is in units of emu/mol and d is the molar density of the compound in units of mol/cm^3. T_c for $LaPt_4Ge_{12}$ is 8 K, and it is suppressed with increasing x down to 4.3 K for $x = 1$, consistent with reported literature for the end-member compounds [2,3]. The volume fraction, v, is consistently near -1 for all x. This is evidence that the sample completely expels magnetic fields and is consistent with bulk superconductivity.

Specific heat divided by temperature $C(T)/T$ versus T plots for $La_{1-x}Ce_xPt_4Ge_{12}$ ($x = 0$, 0.05, and 0.1) and for $La_{0.8}Th_{0.2}Pt_4Ge_{12}$ are displayed in Fig. 6(a). T_c was determined from idealized equal entropy conserving constructions about the specific heat jump associated with superconductivity as seen for $La_{0.95}Ce_{0.05}Pt_4Ge_{12}$ in the inset of Fig. 6(a). In $La_{1-x}Ce_xPt_4Ge_{12}$, T_c was rapidly suppressed with increasing x: from $T_c = 8.3$ K for $x = 0$ down to $T_c = 3.2$ K for $x = 0.1$. For $La_{0.8}Th_{0.2}Pt_4Ge_{12}$, only a small decrease in T_c was observed, shifting down to $T_c = 7.3$ K.

Linear fits using the equation $C(T)/T = \gamma + \beta T^2$ were performed on the specific heat data from the lowest temperature in the normal state up to temperatures as high as linear fits were possible to determine the Sommerfeld coefficient γ and Debye temperature Θ_D. The coefficient of the phonon contribution to the specific heat β is related to Θ_D by the relation $\Theta_D = [1944 \times (n/\beta)]^{1/3}$ K, where $n = 17$ is the number of atoms in the formula unit. The electronic contribution to specific heat γ exhibits a moderate increase with initial Ce substitution where $\gamma = 50$ mJ/mol K^2 for $x = 0$
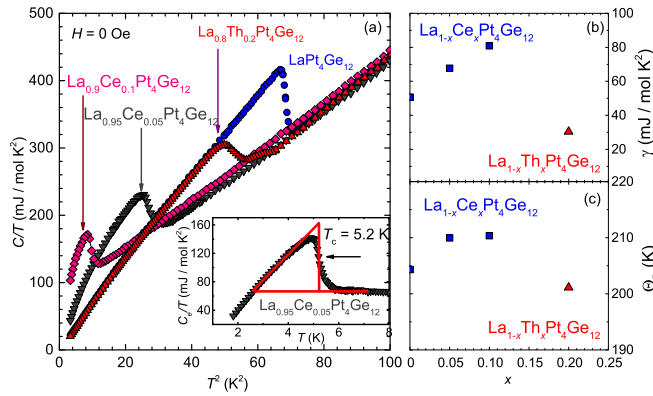
FIG. 6. (a) Specific heat divided by temperature $C(T)/T$ versus T^2 for $La_{1-x}Ce_xPt_4Ge_{12}$ ($x = 0, 0.05,$ and 0.1) and $La_{0.8}Th_{0.2}Pt_4Ge_{12}$ down to 2 K in zero magnetic field. The superconducting critical temperature T_c is suppressed with increasing x, with Ce substitution having a more pronounced effect than Th substitution. T_c values were determined from idealized equal entropy constructions fitted to the electronic contribution to specific heat, C_e/T, as shown in the inset for $La_{0.95}Ce_{0.05}Pt_4Ge_{12}$. Linear fits were performed on the C/T data plotted versus T^2 in the lowest-temperature regions in the normal state to determine the Sommerfeld cofficient γ and the Debye temperature Θ_D; these quantities are plotted in (b) and (c), respectively.

and reaches 80 mJ/mol K^2 for $x = 0.1$, close to the reported values of $\gamma \sim 100$ mJ/mol K^2 for CePt$_4$Ge$_{12}$ [9,13]. Thorium substitution results in a slight suppression of γ, where $\gamma = 30$ mJ/mol K^2 for La$_{0.8}$Th$_{0.2}$Pt$_4$Ge$_{12}$, as shown in Fig. 6(b). Θ_D appears to be insensitive to Ce or Th substitution, fluctuating less than 5% from $\Theta_D = 204$ K for $x = 0$, as seen in Fig. 6(c).

Interestingly, negative curvature was observed in the C/T versus T^2 data as $T \rightarrow 0$ K for La$_{1-x}$Ce$_x$Pt$_4$Ge$_{12}$ with $x \geqslant 0.05$. To investigate this behavior, the electronic contribution to the specific heat $C_e(T)$ was determined by subtracting the phonon contribution from $C(T)/T$ and plotting as $\log(C_e(T)/\gamma T_c)$ versus T_c/T in Fig. 7(a) for La$_{1-x}$Ce$_x$Pt$_4$Ge$_{12}$ and (b) for La$_{1-x}$Th$_x$Pt$_4$Ge$_{12}$. The data sets were offset for clarity. The solid lines represent fits to each data set. For La$_{1-x}$Ce$_x$Pt$_4$Ge$_{12}$, $C_e(T)$ for the samples with $x = 0.05$ and 0.1 is well described by an exponential temperature dependence of the form $be^{-(\Delta/T)}$, where b is a fitting parameter and Δ represents the superconducting energy gap. Best fit values for b were roughly 9.8 and 7.3 for $x = 0.05$ and 0.1, respectively. The best fit values were $\Delta/T_c = 1.52$ and 1.38 for $x = 0.05$ and 0.1, respectively; while the values of Δ/T_c could vary depending on the fitting range [30], the exponential behavior is still evidence for BCS superconductivity. Attempts to fit $C_e(T)$ data for $x = 0$ with the function $be^{-(\Delta/T)}$ were unsuccessful. However, fits using a power-law function of the form cT^n, where c is a fitting parameter, were found to describe $C_e(T)$ versus T for $x = 0$ very well, where $n = 2.5$. The change from cT^n to $be^{-(\Delta/T)}$ temperature dependencies may be explained by a transition from a multiband superconductor to a single-band isotropic s-wave superconductor. $C_e(T) \sim T^n$ behavior is also expected for superconductors with nodes in the energy gap with $n = 2$ for line nodes and $n = 3$ for point nodes [29], while $C(T) \sim e^{-(\Delta/T)}$ behavior is expected for single-band isotropic s-wave superconductors. It should be
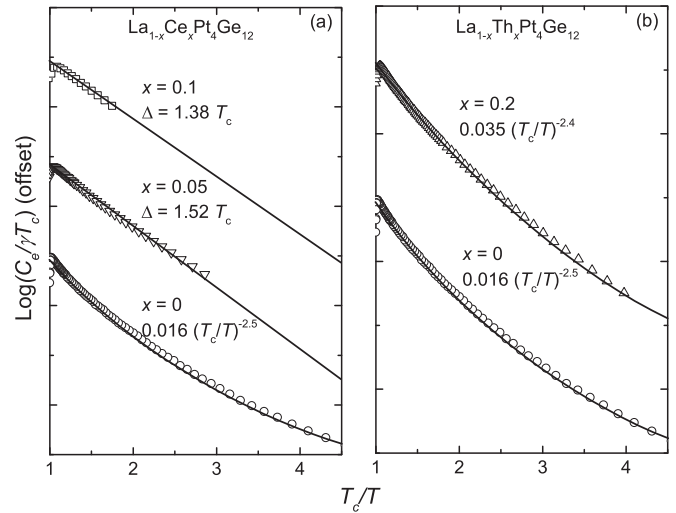

FIG. 7. (a) and (b) The electronic contribution to specific heat plotted as $\log(C_e/\gamma T_c)$ versus T_c/T for La$_{1-x}$Ce$_x$Pt$_4$Ge$_{12}$ and La$_{1-x}$Th$_x$Pt$_4$Ge$_{12}$, respectively. The data sets were offset for clarity. For the La$_{1-x}$Ce$_x$Pt$_4$Ge$_{12}$ samples, the specific heat data are well described by an exponential temperature dependence of the form $e^{-\Delta/T}$, which is the expected behavior for an isotropic superconducting energy gap. However, the LaPt$_4$Ge$_{12}$ and La$_{0.8}$Th$_{0.2}$Pt$_4$Ge$_{12}$ data exhibit a power-law T^n temperature dependence, where $n \sim 2.5$. This result may be consistent with multiband superconductivity.

noted that this type of analysis based on the temperature-dependence of the specific heat is believed to be valid at low temperatures (i.e., $T \ll T_c$) [29,30]. However, our results, including the change of the temperature-dependence of the specific heat and the rapid initial suppression of T_c, are quite similar to those observed in the Pr$_{1-x}$Ce$_x$Pt$_4$Ge$_{12}$ system [9]; this matter has been further investigated by a recent study of the low-temperature specific heat, confirming a crossover in the superconducting gap structure [31]. Combining these factors, we believe that the change in the temperature-dependence of the specific heat is very likely intrinsic to La$_{1-x}$Ce$_x$Pt$_4$Ge$_{12}$. Noninteger values of n can be due to the contributions to specific heat from multiple superconducting gaps, as was observed in PrPt$_4$Ge$_{12}$ [8]. Our results suggest that multiband superconductivity may also occur in LaPt$_4$Ge$_{12}$ as $C(T)$ for this compound varies as $T^{2.5}$ for $T < T_c$, which is consistent with a recent tunnel-diode-oscillator (TDO) and transverse-field muon-spin rotaion (TF-μSR) spectroscopy measurements on LaPt$_4$Ge$_{12}$, suggesting marginal two-gap superconductivity in LaPt$_4$Ge$_{12}$ [32]. A nonintegral value of n for Ce substitution may indicate that the system has been driven to single-band conventional superconductivity. The cT^n behavior of LaPt$_4$Ge$_{12}$ was preserved with $n = 2.4$ for La$_{0.8}$Th$_{0.2}$Pt$_4$Ge$_{12}$.

IV. DISCUSSION

The T_c versus x curve for La$_{1-x}$Ce$_x$Pt$_4$Ge$_{12}$ (blue symbols), derived from $\rho(T)$, $M(T)/H$, and $C(T)$, is shown in Fig. 8. Dashed lines in the figure are guides to the eye. The T_c versus x curve for Pr$_{1-x}$Ce$_x$Pt$_4$Ge$_{12}$ (red symbols) reported in Ref. [9] is also shown for comparison. Displayed in the inset is the T_c versus x curve for La$_{1-x}$Th$_x$Pt$_4$Ge$_{12}$. In La$_{1-x}$Ce$_x$Pt$_4$Ge$_{12}$, the
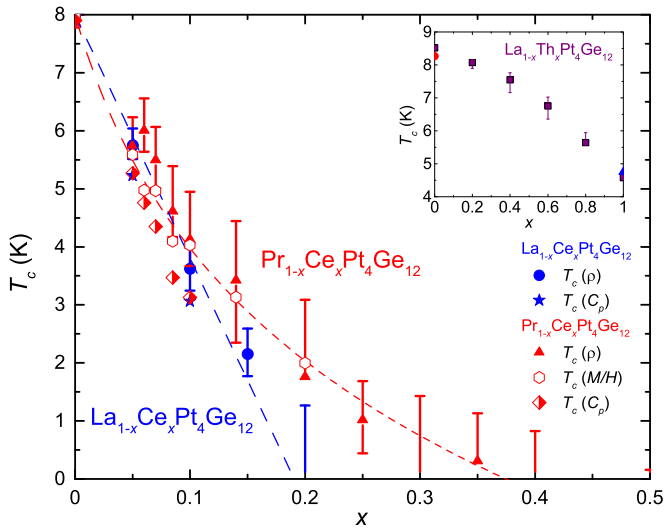
FIG. 8. Plots of the superconducting transition temperature, T_c versus Ce concentration x for $La_{1-x}Ce_xPt_4Ge_{12}$ (blue symbols) and, for comparison, $Pr_{1-x}Ce_xPt_4Ge_{12}$ (red symbols) (Ref. [9]). The dashed lines are guides to the eye. The suppression of T_c with increasing x for $La_{1-x}Ce_xPt_4Ge_{12}$ is greater than in $Pr_{1-x}Ce_xPt_4Ge_{12}$. Whereas the T_c versus x curve for $La_{1-x}Ce_xPt_4Ge_{12}$ is nearly linear, the T_c versus x curve for $Pr_{1-x}Ce_xPt_4Ge_{12}$ exhibits positive curvature. Shown in the inset is the T_c versus x curve for $La_{1-x}Th_xPt_4Ge_{12}$ (purple squares). The response of T_c with increasing x is smooth and continuous. The reported T_c values for $LaPt_4Ge_{12}$ (Ref. [13]) and $ThPt_4Ge_{12}$ (Ref. [3]) are added as a red circle and blue triangle for reference.

initial rate of suppression of T_c, $(dT_c/dx)_{x=0} = -0.4$ K/at. % Ce, is much larger in magnitude than $(dT_c/dx)_{x=0} = -0.04$ K/at. % Th for $La_{1-x}Th_xPt_4Ge_{12}$. Because of the positive curvature of T_c versus x in $Pr_{1-x}Ce_xPt_4Ge_{12}$, we were only able to approximate $(dT_c/dx)_{x=0}$ for $x \lesssim 0.1$ which yields $(dT_c/dx)_{x=0} \sim -0.4$ K/at. % Ce, close to the value obtained for $La_{1-x}Ce_xPt_4Ge_{12}$. The series $La_{1-x}Ce_xPt_4Ge_{12}$ was found to exhibit a rapid and almost linear suppression of T_c with increasing Ce concentration, which extrapolated to 0 K near $x \approx 0.2$. While Ce substitution at low x produces a similar depression of T_c for both $La_{1-x}Ce_xPt_4Ge_{12}$ and $Pr_{1-x}Ce_xPt_4Ge_{12}$, at higher Ce concentrations, the T_c versus x curve for $Pr_{1-x}Ce_xPt_4Ge_{12}$ develops strong positive curvature and appears to extrapolate to 0 K at $x \approx 0.4$, roughly twice the value of x where T_c vanishes for $La_{1-x}Ce_xPt_4Ge_{12}$.

The T_c versus x curves for the $Ln_{1-x}Ce_xPt_4Ge_{12}$ ($Ln = La$ and Pr) systems shown in Fig. 8 reveal that the rate of depression of T_c with Ce concentration is similar for the two systems, both of which have values of $T_c \approx 8$ K at $x = 0$, for $x \lesssim 0.1$, and is significantly weaker for $Pr_{1-x}Ce_xPt_4Ge_{12}$ than $La_{1-x}Ce_xPt_4Ge_{12}$ for $0.1 \lesssim x \lesssim 0.2$. This reveals that the Ce substituents produce stronger superconducting electron pair breaking in the $LaPt_4Ge_{12}$ compound, in which the electronic correlations are relatively weak and the superconductivity is conventional [11,12], than in the $PrPt_4Ge_{12}$ compound, where the electronic correlations are stronger and the superconductivity is unconventional (e.g., superconductivity breaks time-reversal symmetry) [4–10]. Since the $CePt_4Ge_{12}$ end member compound is also a correlated electron system [11],

the electronic correlations associated with the Ce solutes apparently have a stronger pair breaking effect on the conventional superconductivity exhibited by the $LaPt_4Ge_{12}$ parent compound than on the unconventional superconductivity displayed by the $PrPt_4Ge_{12}$ parent compound. The shapes of the T_c versus x curves for the $Ln_{1-x}Ce_xPt_4Ge_{12}$ ($Ln = La$ and Pr) systems are reminiscent of metallic host metals that exhibit conventional superconductivity containing transition metal, lanthanide, and actinide solute ions with partially-filled d- or f-electron shells in which the normal ground state at superconducting temperatures is nonmagnetic [33]. In these systems, a characteristic temperature T_0 associated with spin fluctuations, valence fluctuations, or the Kondo effect separates high-temperature local moment behavior, characterized by a Curie-Weiss law, and low-temperature nonmagnetic behavior, reflected in a magnetic susceptibility that approaches a finite value as $T \to 0$ K. When T_0 is much larger than the T_c of the superconducting host metal (T_{c0}), the initial rate of depression of T_c can be quite large and have pronounced positive curvature, similar to that observed for $Pr_{1-x}Ce_xPt_4Ge_{12}$. This behavior is well established, and exemplary systems in which it has been observed include the $Al_{1-x}Mn_x$ [34], $Th_{1-x}Ce_x$ [35], and $Th_{1-x}U_x$ [36] systems, where the Al and Th host metals are conventional superconductors. If one assumes that the temperature at which the magnetic susceptibility of the $Ln_{1-x}Ce_xPt_4Ge_{12}$ ($Ln = La$ and Pr) samples attains a maximum value is of the order of the characteristic temperature T_0, then these systems are in the limit that $T_0 \gg T_{c0}$ (e.g., $T_0 \sim 50$–100 K for both the La- and Pr-based systems). It is tempting to compare the T_c versus x data with theories of superconductivity in host-impurity systems that display the Kondo effect, such as the theory of Müller-Hartmann and Zittartz [37]. However, these theories are based on the host metal being a simple one-band conventional BCS superconductor and for noninteracting paramagnetic impurities. The $Ln_{1-x}Ce_xPt_4Ge_{12}$ ($Ln = La$ and Pr) compounds have complex Fermi surfaces with multiple sheets that apparently lead to multiband superconductivity [6–9], large Ce solute concentrations in which the interactions between Ce ions increase with Ce concentration, and conventional superconductivity displayed by the La-based compound [11,12] and unconventional superconductivity exhibited by the Pr-based compound [4–10].

Previous studies show that $C(T)$ for $ThPt_4Ge_{12}$ exhibits a T^3 temperature dependence for $T < T_c$, which may suggest that there are point nodes in the superconducting energy gap [16]. If this interpretation is correct, the superconductivity exhibited by $ThPt_4Ge_{12}$ could be unconventional. Therefore chemical substitution between $ThPt_4Ge_{12}$ and $LaPt_4Ge_{12}$, might be expected to result in a pronounced minimum in $T_c(x)$ due to competing superconducting phases as was observed in studies of the filled skutterudite system $PrOs_{4-x}Ru_xSb_{12}$ [18,19,38]. Instead, we observe a smooth and continuous T_c versus x curve for $La_{1-x}Th_xPt_4Ge_{12}$, showing no evidence for competing superconducting phases. One possible explanation for this behavior is that both $LaPt_4Ge_{12}$ and $ThPt_4Ge_{12}$ may be multiband superconductors, with each band exhibiting conventional BCS superconductivity. Band-structure calculations demonstrate that $ThPt_4Ge_{12}$ exhibits multiple Fermi surface sheets, which is a requirement

for multiband superconductivity [17]. Additionally, the T^3 temperature-dependence of the specific heat was used to suggest point nodes in the energy gap; however, the power-law temperature dependence of $C(T)$ can also be evidence of multiband superconductivity, as was suggested for $PrPt_4Ge_{12}$ [8]. With respect to $LaPt_4Ge_{12}$, band-structure calculations also predict multiband crossings at the Fermi energy, E_F [6]. When we combine this with the results from the present study, which show that the specific heat of $LaPt_4Ge_{12}$ displays a power-law temperature-dependence in the superconducting state and that the response of superconductivity in $LaPt_4Ge_{12}$ to Ce substitution is similar to that in the potential multiband superconductor $PrPt_4Ge_{12}$ [6–9], there is mounting evidence for multiband superconductivity in $LaPt_4Ge_{12}$. The apparent similarity of the superconducting states of $LaPt_4Ge_{12}$ and $ThPt_4Ge_{12}$ reinforces this possibility. However, further work will be necessary to definitively address the nature of the superconducting energy gap(s) in $LaPt_4Ge_{12}$ [29,39].

V. CONCLUDING REMARKS

The $La_{1-x}Ce_xPt_4Ge_{12}$ and $La_{1-x}Th_xPt_4Ge_{12}$ systems were studied by means of electrical resistivity, magnetization, and specific heat measurements. The broad maxima in the $\chi(T)$ data for $CePt_4Ge_{12}$ were suppressed with increasing La concentrations, both in temperature and amplitude, which may be due to weakening of the Ce-Ce interactions with increasing La concentration. Superconductivity in the $La_{1-x}Ce_xPt_4Ge_{12}$ system was rapidly suppressed with increasing Ce concentration, with no evidence for superconductivity down to 1.1 K for $x > 0.2$. The suppression of T_c in $La_{1-x}Ce_xPt_4Ge_{12}$ is significantly more rapid than previously observed in $Pr_{1-x}Ce_xPt_4Ge_{12}$, supporting an interpretation that the superconductivity observed in these two systems is different in nature. Specific heat measurements in the superconducting state of $La_{1-x}Ce_xPt_4Ge_{12}$ revealed a change from a power law to exponential temperature dependence, similar to the results from a study on $Pr_{1-x}Ce_xPt_4Ge_{12}$; this may suggest that, although superconductivity in $LaPt_4Ge_{12}$ is conventional, while it is unconventional in $PrPt_4Ge_{12}$, both may exhibit a crossover from multiband superconductivity to single-band superconductivity with Ce substitution. In contrast, $LaPt_4Ge_{12}$ and $ThPt_4Ge_{12}$ appear to exhibit the same type of superconductivity as evidenced by the continuous and smooth behavior of T_c with increasing x in $La_{1-x}Th_xPt_4Ge_{12}$ and the power-law temperature dependence of specific heat in the superconducting state.

[1] E. Bauer, A. Grytsiv, X. Chen, N. Melnychenko-Koblyuk, G. Hilscher, H. Kaldarar, H. Michor, E. Royanian, G. Giester, M. Rotter *et al.*, Phys. Rev. Lett. **99**, 217001 (2007).

[2] R. Gumeniuk, W. Schnelle, H. Rosner, M. Nicklas, A. Leithe-Jasper, and Y. Grin, Phys. Rev. Lett. **100**, 017002 (2008).

[3] E. Bauer, X.-Q. Chen, P. Rogl, G. Hilscher, H. Michor, E. Royanian, R. Podloucky, G. Giester, O. Sologub, and A. P. Goncalves, Phys. Rev. B **78**, 064516 (2008).

[4] A. Maisuradze, M. Nicklas, R. Gumeniuk, C. Baines, W. Schnelle, H. Rosner, A. Leithe-Jasper, Y. Grin, and R. Khasanov, Phys. Rev. Lett. **103**, 147002 (2009).

[5] A. Maisuradze, W. Schnelle, R. Khasanov, R. Gumeniuk, M. Nicklas, H. Rosner, A. Leithe-Jasper, Y. Grin, A. Amato, and P. Thalmeier, Phys. Rev. B **82**, 024524 (2010).

[6] Y. Nakamura, H. Okazaki, R. Yoshida, T. Wakita, H. Takeya, K. Hirata, M. Hirai, Y. Muraoka, and T. Yokoya, Phys. Rev. B **86**, 014521 (2012).

[7] S. Chandra, L. S. Chattopadhyay, and S. B. Roy, Philos. Mag. **92**, 3866 (2012).

[8] J. L. Zhang, Y. Chen, L. Jiao, R. Gumeniuk, M. Nicklas, Y. H. Chen, L. Yang, B. H. Fu, W. Schnelle, H. Rosner *et al.*, Phys. Rev. B **87**, 064502 (2013).

[9] K. Huang, L. Shu, I. K. Lum, B. D. White, M. Janoschek, D. Yazici, J. J. Hamlin, D. A. Zocco, P.-C. Ho, R. E. Baumbach *et al.*, Phys. Rev. B **89**, 035145 (2014).

[10] I. Jeon, K. Huang, D. Yazici, N. Kanchanavatee, B. D. White, P.-C. Ho, S. Jang, N. Pouse, and M. B. Maple, Phys. Rev. B **93**, 104507 (2016).

[11] M. Toda, H. Sugawara, K.-i. Magishi, T. Saito, K. Koyama, Y. Aoki, and H. Sato, J. Phys. Soc. Jpn. **77**, 124702 (2008).

[12] F. Kanetake, H. Mukuda, Y. Kitaoka, H. Sugawara, K. Magishi, K. M. Itoh, and E. E. Haller, Physica C **470**, S703 (2010).

[13] R. Gumeniuk, K. O. Kvashnina, W. Schnelle, M. Nicklas, H. Borrmann, H. Rosner, Y. Skourski, A. A. Tsirlin, A. Leithe-Jasper, and Y. Grin, J. Phys.: Condens. Matter **23**, 465601 (2011).

[14] R.-M. Galéra, C. Opagiste, M. Amara, M. Zbiri, and S. Rols, J. Phys.: Conf. Ser. **592**, 012011 (2015).

[15] V. H. Tran, A. D. Hillier, D. T. Androja, and D. Kaczorowski, J. Phys.: Condens. Matter **22**, 505701 (2010).

[16] D. Kaczorowski and V. H. Tran, Phys. Rev. B **77**, 180504 (2008).

[17] V. H. Tran, B. Nowak, A. Jezierski, and D. Kaczorowski, Phys. Rev. B **79**, 144510 (2009).

[18] N. A. Frederick, T. D. Do, P.-C. Ho, N. P. Butch, V. S. Zapf, and M. B. Maple, Phys. Rev. B **69**, 024523 (2004).

[19] M. B. Maple, Z. Henkie, W. M. Yuhasz, P.-C. Ho, T. Yanagisawa, T. A. Sayles, N. P. Butch, J. R. Jeffries, and A. Pietraszko, J. Magn. Magn. Mater. **310**, 182 (2007).

[20] A. C. Larson and R. B. Von Dreele, General Structure Analysis System (GSAS), Los Alamos National Laboratory Report (2004).

[21] B. H. Toby, J. Appl. Crystallogr. **34**, 210 (2001).

[22] R. Gumeniuk, H. Borrmann, A. Ormeci, H. Rosner, W. Schnelle, M. Nicklas, Y. Grin, and A. Leithe-Jasper, Z. Kristallogr. **225**, 531 (2010).

[23] B. D. White, K. Huang, and M. B. Maple, Phys. Rev. B **90**, 235104 (2014).

[24] D. A. Gajewski, N. R. Dilley, E. D. Bauer, E. J. Freeman, R. Chau, M. B. Maple, D. Mandrus, and B. C. Sales, J. Phys.: Condens. Matter **10**, 6973 (1998).

[25] M. Nicklas, S. Kirchner, R. Borth, R. Gumeniuk, W. Schnelle, H. Rosner, H. Borrmann, A. Leithe-Jasper, Y. Grin, and F. Steglich, Phys. Rev. Lett. **109**, 236405 (2012).

[26] N. Takeda and M. Ishikawa, J. Phys.: Condens. Matter **13**, 5971 (2001).

[27] H. G. Lukefahr, O. O. Bernal, D. E. MacLaughlin, C. L. Seaman, M. B. Maple, and B. Andraka, Phys. Rev. B **52**, 3038 (1995).

[28] M. B. Maple, E. D. Bauer, V. S. Zapf, and P.-C. Ho, Physica B **318**, 68 (2002).

[29] M. Sigrist and K. Ueda, Rev. Mod. Phys. **63**, 239 (1991).

[30] G. Gladstone, M. A. Jensen, and J. R. Schrieffer, in *Superconductivity*, edited by R. D. Parks (Marcel Dekker, New York, 1969), Vol. 2.

[31] Y. P. Singh, R. B. Adhikari, S. Zhang, K. Huang, D. Yazici, I. Jeon, M. B. Maple, M. Dzero, and C. C. Almasan, arXiv:1607.03563.

[32] J. L. Zhang, G. M. Pang, L. Jiao, M. Nicklas, Y. Chen, Z. F. Weng, M. Smidman, W. Schnelle, A. Leithe-Jasper, A. Maisuradze *et al.*, Phys. Rev. B **92**, 220503 (2015).

[33] M. B. Maple, App. Phys. **9**, 179 (1976).

[34] J. G. Huber and M. B. Maple, Solid State Commun. **8**, 1987 (1970).

[35] J. G. Huber, W. A. Fertig, and M. B. Maple, Solid State Commun. **15**, 453 (1974).

[36] M. B. Maple, J. G. Huber, B. R. Coles, and A. C. Lawson, J. Low Temp. Phys. **3**, 137 (1970).

[37] E. Müller-Hartmann and J. Zittartz, Phys. Rev. Lett. **26**, 428 (1971).

[38] L. Shu, D. E. MacLaughlin, Y. Aoki, Y. Tunashimia, Y. Yonezawa, S. Sanada, D. Kikuchi, H. Sato, R. H. Heffner, W. Higemoto *et al.*, Phys. Rev. B **76**, 014527 (2007).

[39] R. Balian and N. R. Werthamer, Phys. Rev. **131**, 1553 (1963).